



33 achieved by considering its survival conditions. The most dominant environmental forces that
34 dictates this design of structure is due to the maximum probable wave height of a site of
35 interest (Massel, 1978).

36 Depending on the importance and life span of the structure, the return period of the extreme
37 events could be selected as 30 years or 100 years. The lesser would be associated with lesser
38 wave height but more risk and vice versa. It demands a better understanding of hydrodynamic
39 characteristics of local wave environment, especially the extreme conditions. In the design of
40 any marine structures, the first step is the extreme wave analysis for the determination of
41 design wave heights with certain return periods (Goda, 2000). Estimation of appropriate
42 design values indicate the level of protection and the scale of investment during the
43 construction of structure.

44 Fundamentally, extreme values are scarce and are necessarily outside the range of the
45 available observations, implying that an extrapolation from the observed sea states to
46 unknown territories is required. An estimate of anticipated wave height can be furnished
47 using historical wave hind-cast data or field observed data with the help of various
48 distribution models, which enable extrapolation under the Extreme value theory framework
49 (Goda, 2000; Coles, 2001; Caires, 2011). Ferreira and Soares, 2000 suggested that the
50 estimation of extreme values should rely on methods based on extreme value theory which
51 makes use of the largest of the observations in the sample. Coles, 2001 obtained the detailed
52 statistical results of extreme value prediction using the annual maximum (AM) (Castillo,
53 1988) and Peaks Over Threshold (POT) (Ferreria and Soares, 1998) sampled observations.
54 Caires, 2011 rigorously compared the commonly used extreme value statistical methods (like
55 GEV and GPD) with different parameter estimation methods for combination of different
56 data sampling techniques.

57 Another approach that may be applied starting from a wave data time series is that of
58 equivalent storm models (Boccotti 1986, 2000; Arena and Pavone, 2009; Fedele and Arena,
59 2010; Laface and Arena, 2016) which is based on the concept of sea storm. Specifically
60 these models consist in substituting the sequence of sea storms at a given site (actual sea)
61 with a sequence of equivalent storms (equivalent sea) from a statistical perspective. The
62 equivalent storms have very simple geometric shapes such as triangular (Boccotti 1986,
63 2000; Arena and Pavone, 2009), power (Fedele and Arena, 2010) or exponential (Laface and
64 Arena, 2016). Depending on the shape the related model gives analytical or numerical



65 solution for the calculation of the return period $R(H_s > h)$ of a sea storm whose maximum H_s is
66 greater than a given threshold h . Specifically the triangular and exponential equivalent storm
67 models give closed form solution for $R(H_s > h)$, while the Equivalent power storm model
68 requires numerical calculation. In the paper the Equivalent Triangular (ETS) model is
69 utilized.

70 The accuracy of any methodology for extreme values significantly depends on the length of
71 the recorded time series data. It is believed that measurements from wave rider buoy offer the
72 most reliable long historical record. However, the availability of such buoy data is limited to
73 a certain specific locations, mainly in the northern hemisphere. At a particular location of
74 interest, the availability of buoy data is usually scarce, and often there will be no data. The
75 oceanographic community has recognized the hind-casts with ocean wave models to
76 complement the limited buoy observational records.

77 In the recent years, the performance of wave models has appreciably improved, with better
78 quality of the wind fields and enhancement in numerical wave modeling. The meteorological
79 centres like European Centre for Medium-Range Weather Forecasts (ECMWF), Australian
80 Bureau of Meteorology and Meteo-France that operate global wave models are currently
81 using altimeter wind data for data assimilation purposes. The process combines numerical
82 wave model and observations of diverse sorts in the best possible ways to generate a
83 consistent, global estimate of the various atmospheric, wave and oceanographic parameters.
84 At present, in numerous meteorological centres, wind and wave simulated data are
85 assimilated on a daily basis.

86 The simulated hindcast data have been adopted in numerous studies for the estimation of
87 extreme wave conditions. Teena et al., 2012 applied a generalized extreme value distribution
88 and generalized Pareto distribution to the 31 years assimilated wave hindcast data based on
89 MIKE-21, a spectral wave model for a location in the eastern Arabian sea and extracted
90 extreme wave for several return periods. Li et al., 2016 used a third generation wave model,
91 WAMC4 and simulated 35 years of wave hindcast data from two sets of reanalysis wind data,
92 NCEP and ECMWF. In their study, Pearson-III distribution method is used to analyse the
93 extreme wave climate in the East China seas. Polnikov and Gomorev, 2015 proposed to use
94 the extrapolation of polynomial approximation constructed for the shorter part of the tail of
95 probability function to estimate the return values of wind speed and wind-wave height. The



96 wave field was computed from wind-wave model, WAM-C4M from ECMWF global
97 atmospheric reanalysis ERA-interim wind field data.

98 Even though several studies have been carried out, the study on the identification of the most
99 suitable approach for estimating extreme wave heights for a particular source of assimilated
100 wave hindcast data is still lacking. In the present study, the investigation of different existing
101 approaches and models is carried to assess its application and reliability for the Indian
102 domain. Increased uncertainty in the model outputs questions the reliability of the estimation
103 model, which is an important issue. Thus, the present study introduces a statistical approach
104 to validate the reliability of the design wave height return values resulting from a particular
105 extreme wave estimation method by considering variability criterion as measured maximum
106 value. The variation in the extreme value estimates of the ERA-interim data and the buoy
107 data for different estimation models is also considered and examined. The objective of the
108 present study is to identify a robust extreme wave height estimation method for Indian
109 domain using global atmospheric reanalysis ERA-interim wave hindcast data.

110 **2. Datasets**

111 **2.1 Study Locations**

112 Four offshore locations along the Indian coast (Fig.1) are considered. The selection of these
113 particular locations is based on their distance from the nearest coast and the water depth, two
114 each on east and west coasts of the Indian peninsula. Both deep and shallow water locations
115 are chosen to examine the application of the estimation model based on water depth.

116 The projected estimates using ERA-Interim data are compared with those obtained from data
117 from various buoys to validate the performance of ERA-Interim data in extreme wave
118 analysis. The choice of the locations was according to the size of wave data that were
119 available. Further, two locations in North America, National Data Buoy Center Station 44005
120 in Gulf of Maine, National Data Buoy Center Station 46050 West of Newport and one of the
121 most energetic sites in the coasts of Central Mediterranean Sea (Liberti et al., 2013;
122 Vicinanza et al., 2013; Arena et al., 2015) from the Italian buoys network (RON) locations,
123 Alghero (West coast of Sardinia Island) are considered. A comprehensive comparison has
124 been carried out by extracting the ERA-Interim data of resolution $0.125^{\circ} \times 0.125^{\circ}$ nearest to
125 the selected buoy locations. The coordinates, period of data availability, interval and number
126 of data points for these locations are presented in Table 1.



127 **2.2 Wave Data**

128 **2.2.1 ERA-Interim data**

129 ERA-Interim data is produced by the ECMWF, which is a global atmospheric reanalysis from
130 1979, continuously updated in real time and is one among the most recent re-analysis data
131 available (Berrisford et al., 2009). ERA-Interim is the first to perform re-analysis using
132 adaptive and fully automated bias corrections of observations (Dee and Uppala, 2008). The
133 parameters such as significant wave height (H_s), mean wave direction and mean wave period
134 can be obtained with 6-hourly fields covering the whole globe, with the best space resolution
135 of $0.125^\circ \times 0.125^\circ$.

136 There have been several studies comparing the values of H_s between ERA-Interim dataset and
137 buoy data at different locations around the world to evaluate the model performance. It has
138 been found that at certain locations in the Arabian sea, the maximum H_s based on ERA
139 dataset in deep water is about 15% less than that of buoy measured data, whereas, in shallow
140 waters, ERA dataset over predicts the maximum H_s by about 9% (Shanas and Kumar, 2014).
141 The under prediction in deep water suggests that extreme events attained mainly during
142 cyclones are difficult to be captured by the model. The results show that H_s of model data set
143 are reliable in both deep and shallow water locations with a good degree of accuracy. The
144 estimates in this study are based on ERA-Interim wave hind cast data, covering a period of 36
145 years (1979-2014). For nearest intersection buoy locations, the data period was selected based
146 on buoy data availability.

147 **2.2.2 Buoy data**

148 The most reliable data for significant wave height are from the buoy measurements. The
149 available length of buoy data is usually limited and the data prior to 1978 is scanty. The
150 available buoy data further requires significant quality control on account of large gaps of
151 missing data and outlier, flagship measurements. In the paper data from two different buoys
152 networks are processed: RON (Rete Ondametrica Nazionale) Italian network and the
153 National Oceanic and Atmospheric Administration's National Data Buoys Center (NOAA-
154 NDBC).

155 The Italian buoys network (RON) started measurements in 1989, with 8 directional buoys
156 located off the coasts of Italy. Later it has reached the number of 15 buoys moored in deep
157 water. For each record, the data of significant wave height, peak and mean period and
158 dominant direction are given.



159 The NOAA manages the NDBC, which consists of many buoys moored along the US coasts,
160 both in the Pacific Ocean and in the Atlantic Ocean. Some buoys were moored in the late
161 1970s, so that more than 35 years of data are available. The historical wave data give hourly
162 significant wave height, peak and mean period. The NOAA buoy observations are readily
163 available which are of proven quality. The measurements have passed through quality control
164 by NOAA. It is however always recommended to perform some basic quality checks.

165 The return value estimates acquired from the ERA-Interim data are compared with that of
166 NDBC Stations 44005, 46050 and at Alghero along the coast of Central Mediterranean Sea.
167 Table-1 provides the coordinates and data details of these buoy stations. ERA-Interim wave
168 hindcast data has been used to assess the estimates in Indian waters.

169 **3. Extreme wave height Estimation Methods**

170 **3.1 General**

171 The estimation models used in this study to obtain extreme wave return values include the
172 generalised extreme value (GEV) and the generalised Pareto distribution (GPD), which are
173 currently being adopted for the standard practice in mainstream extreme statistics. Each
174 distribution was fit to the data using the Maximum likelihood method (MLE) and the
175 Probability weighted moments method (PWM). Further, new polynomial approximation
176 model prescribed by Polnikov and Gomorev, 2015 and Equivalent Triangular storm model
177 (Boccotti, 2000) based on the concept of replacing the sequence of actual storms extrapolated
178 from a given time series of H_s with a sequence of equivalent triangular storms are used.

179

180 **3.2 Generalised extreme value distribution model**

181 According to extreme value theory, to form a valid distribution, the sampled observations
182 should be independent which would mean that successive observations should not be
183 correlated with one another and identically distributed (Goda, 2000). In general, for the
184 sampling of data to be used for extreme wave analysis three different approaches are
185 available. The first approach uses all the recorded data of H_s during a number of years and fits
186 a cumulative distribution to this data. This approach is called the initial distribution method
187 (IDM). For the other two approaches, only the peaks of wave heights are engaged. The
188 method of block maxima consists of partitioning recorded data in blocks, where in, maximum
189 value of each block is considered. Normally a block could be chosen as one year (Lionello et
190 al., 1992). The POT (Peaks Over Threshold) method, consists of the peaks of clustered data
191 exceeding over a given threshold. IDM observations violate the conditions of identity and



192 independence in distribution, which invalidates the application of the common statistical
 193 methods as well as the definition of return values (Anderson et al., 2001). The annual maxima
 194 method and POT method both satisfy the obligatory of independency.
 195 According to theory of the generalized extreme value (GEV) distribution, the sample has
 196 been selected by means of annual maxima (AM) method.

197 The generalized extreme value (GEV) distribution has the cumulative distribution function
 198 (CDF) as:

$$199 \quad GEV(x; \mu, \sigma, \xi) = \begin{cases} \exp\left(-\left(1 - \xi\left(\frac{x-\mu}{\sigma}\right)\right)^{\frac{1}{\xi}}\right), & \text{for } \xi \neq 0 \\ \exp\left(-\exp\left(\frac{-(x-\mu)}{\sigma}\right)\right), & \text{for } \xi = 0 \end{cases} \quad (1)$$

200 where, μ , σ and ξ represent the location, scale and shape parameters of distribution,
 201 respectively and within the range of $-\infty < \mu < \infty$, $\sigma > 0$ and $-\infty < \xi < \infty$. By setting the shape
 202 parameter, ξ , one can obtain the most common distributions like Gumbel ($\xi=0$), Fréchet
 203 ($\xi>0$) and Weibull ($\xi<0$).

204 The 1/T yr wave height return value, X_T based on the GEV distribution model is given as

$$205 \quad X_T = \begin{cases} \mu - \frac{\sigma}{\xi} \left\{ 1 - \left[-\log\left(1 - \frac{1}{T}\right) \right]^{\xi} \right\}, & \text{for } \xi \neq 0 \\ \mu - \sigma \ln\left[-\log\left(1 - \frac{1}{T}\right)\right], & \text{for } \xi = 0 \end{cases} \quad (2)$$

206 3.3 Generalised Pareto distribution model

207 This approach is based on fitting the generalized Pareto distribution (GPD) to the POT
 208 sampled data. The observations in a cluster above the threshold are considered and
 209 calculating return values has been done by taking into account the rate of occurrence of
 210 clusters (Davidson and Smith, 1990; Coles, 2001).

211 The cumulative distribution function of GPD is given as:

$$GPD(x; \mu, \sigma, \xi) = \begin{cases} 1 - \left(1 - \xi\left(\frac{x-\mu}{\sigma}\right)\right)^{\frac{1}{\xi}}, & \text{for } \xi \neq 0 \\ 1 - \exp\left(-\left(\frac{x-\mu}{\sigma}\right)\right), & \text{for } \xi = 0 \end{cases} \quad (3)$$



212 where $0 < x < \infty$, $\sigma > 0$ and $-\infty < \xi < \infty$. where μ is the threshold, scale (σ) and shape (ξ)
 213 parameters. When $\xi = 0$ the GPD is said to amounts to the exponential distribution with mean
 214 σ ; when $\xi > 0$, it is the Pareto distribution; and when $\xi < 0$ it is a special case of the beta
 215 distribution.

216 The 1/T yr wave height return value based on the GPD distribution model X_T , is given as

$$X_T = \begin{cases} \mu + \frac{\sigma}{\xi} \{1 - (\lambda T)^{-\xi}\}, & \text{for } \xi \neq 0 \\ \mu + \sigma \ln(\lambda T) \xi, & \text{for } \xi = 0 \end{cases} \quad (4)$$

217 where, $\lambda = N_u/N$, with N_u being the total number of exceedances above the selected threshold
 218 u and N are the number of years in the record.

219

220 There are several parameter estimation methods for fitting the above candidate distribution
 221 functions to the sampled wave data (Goda, 2000). The method of moments (MM),
 222 probability weighted moments (PWM) method and the maximum likelihood method (MLE)
 223 are more preferred estimation methods since these are more flexible, particularly when the
 224 number of parameters is increased. The MM yields a large bias particularly for small size
 225 samples and this method was not used in the present study. The parameters of the above
 226 distributions are derived according to the methods of maximum likelihood method (MLE)
 227 and probability weighted moments (PWM).

228

229 The threshold selection in GPD analysis is an important practical problem, which is
 230 analogous to the block size in the block maxima approach. The threshold value represents a
 231 compromise between bias and variance. Too low a threshold violates the asymptotic basis of
 232 the GPD model, leading to a bias. Too high a threshold will generate fewer values of excess
 233 to estimate the model, leading to high variance. There is an extensive literature on the attempt
 234 to choose an optimal threshold by Neelamani, 2009; Caires, 2011. In this study, the threshold
 235 selection is based on the Mean residual life plots introduced by Davison and Smith, 1990.

236 The mean residual life plot is based on the theoretical mean of the GPD given as:

$$E[x] = \mu + \frac{\sigma}{1 - \xi}, \text{ for } \xi < 1 \quad (5)$$

238 The mathematical basis for Mean residual life plots method is



239
$$E[X - y | X > y > 0] = \frac{\sigma + \xi y}{1 - \xi}, \text{ for } \xi < 1 \quad (6)$$

240 If X is GPD, then the mean excess over a threshold y (for $y > 0$) with slope $\xi/(1 - \xi)$ is a
 241 linear function of y . Thus, we can draw a plot in which the ordinate is the sample mean of all
 242 excesses over that threshold and the abscissa is the threshold.

243 A mean residual life plot consists in representing points:

244
$$\left\{ \left(\mu, \frac{1}{n} \sum_{i=1}^n x_i, n - \mu \right) : \mu \leq x_{\max} \right\} \quad (7)$$

245 where n is the number of observations ($x_i, i=1,2,\dots,n$) above the threshold μ , and x_{\max} is the
 246 maximum of the observations. According to the Central Limit Theorem, confidence intervals
 247 are added to this mean residual life plot as the empirical mean to be normally distributed.
 248 However, this normality doesn't hold for high threshold as there are less and less excesses.

249 3.4 Polynomial approximation model

250 Polnikov and Gomorev, 2015 proposed to use the extrapolation of polynomial approximation
 251 constructed for the shorter part of the tail of probability function to estimate the return values
 252 of wind speed and wave height.

253 This method involves the construction of an analytical approximation $F_{\text{ap}}(H)$, aimed for its
 254 extrapolation beyond the observed maximum value H_M . The approximation should be
 255 restricted to a shorter domain lying above the uppermost mode of the histogram considered of
 256 the function $F(H)$. The domain suitable for approximation can be determined by the condition

257
$$H_l \leq H \leq H_h \leq H_M \quad (8)$$

258 where H_l and H_h are the lower and the upper edges of the domain of $F(H)$, used for
 259 constructing approximation $F_{\text{ap}}(H)$. The number of points (N_M) considered in the histogram is
 260 $H_M/\Delta H$ and N_S is defined as,

261
$$N_S = (H_M - H_h) / \Delta H \quad (9)$$

262 And the number of points (N_T) used for building approximation $F_{\text{ap}}(H)$ is defined as,

263
$$N_T = (H_h - H_l) / \Delta H + 1 \quad (10)$$



264 The approximation, $F_{ap}(H)$ should be built in the logarithmic coordinates due to few values
265 in the tail of $F(H)$, providing importance to the tail values. It allows to assess the strong
266 variability of the tail of function $F(H)$ near the maximum value of the series, depending on
267 the length of the series. To exclude the application of fixed statistics, the approximation
268 function $F_{ap}(H)$ in the form of a polynomial of degree n , the value of which may vary is
269 considered. The varying n allows obtaining the approximation $F_{ap}(H,n)$ with an accuracy
270 higher than the case of using the fixed statistical distributions.

271 The statistical distribution with the provision function is of the form,

$$272 \quad F_{ap}(H) = \exp \left[\sum_{i=0}^{i=n} a_k H^k \right] \quad (11)$$

273 Once the approximation function, $F_{ap}(H)$ is obtained from Eq.(11), the return value, X_R ,
274 appearing once for N_R years, can be deduced by inverting the formula,

$$275 \quad F(X_R) = \Delta t / 8760 \cdot N_R \quad (12)$$

277 where, Δt is the interval of discrete of data observations.

278 Another, principal features of P-approximation $F_{ap}(W)$ are given as the standard deviation δ
279 (hereinafter, the deviation), defined by the formula:

$$280 \quad \left(\frac{1}{N_T} \cdot \sum_{H_i=H_l}^{H_i=H_h} \left[\ln(F(H_{idp})) - \ln(F(H)) \right]^2 \right)^{1/2} = \delta \quad (13)$$

281 Obviously for, the lesser δ the higher accuracy of approximation can be achieved and it is
282 more preferable.

283 3.5 Equivalent Triangular Storm model

284 The Equivalent Triangular Storm (ETS) model (Boccotti, 2000; Arena and Pavone, 2006,
285 2009) is applied for calculating return values of significant wave height for given thresholds
286 of return period. The ETS approach is based on the assumption that given a sequence of
287 actual storms it may be replaced by an equivalent storm sequence maintaining the same wave
288 risk. The validity of the above assumption is guaranteed by the statistics equivalence between
289 the actual storm and the related Equivalent Triangular (ETS) one. The ETS associated with a



290 given storm is achieved by means of two parameters: the triangle height a and its base b (Fig.
291 2). The former is an intensity parameter and is equaled to the maximum significant wave
292 height during the actual storm, the latter is a duration parameter and it is determined
293 following an iterative procedure imposing the equality between the maximum expected wave
294 heights of actual and triangular storms. It has been experimentally proved that imposing this
295 equality not only the area under the exceedance probability curves of the maximum wave
296 height are the same, but those curves tend to coincide.

297 Considering all these aspects emerges that the actual storm and the ETS sequences (actual
298 and Equivalent Triangular seas) have the same number of storms, each of them characterized
299 by the same maximum significant wave height and the same probability $P(H_{max} > H)$ that the
300 maximum wave height is greater than a fixed threshold H . The considerations above enable
301 to affirm that the return period of a sea storm with given characteristics is the same if
302 calculated starting from the actual storm sequence or the ETSs one. Referring to equivalent
303 triangular sea, an analytical solution for the calculation of the return period $R(H_s > h)$ of a sea
304 storm whose maximum significant wave height is greater than a given threshold h has been
305 developed by Boccotti, 2000.

$$306 \quad R(H_s > h) = \frac{\bar{b}(h)}{hp(H_s = h) + P(H_s > h)} \quad (14)$$

307 Where $\bar{b}(h)$ is the base-height regression function of ETSs, $P(H_s > h)$ is the probability of
308 exceedance of the significant wave height H_s at the considered site and

309 $p(H_s = h) = -\frac{dP(H_s > h)}{dh}$ is the probability density function of H_s .

310 The calculation of return values of H_s by means of Eq. (14) requires the determination of two
311 functions:

- 312 • the base-height regression function, $\bar{b}(h)$ which gives the average value of the base b
313 of ETSs for a given storm height h ;
- 314 • the probability $P(H_s > h)$.

315 The function $\bar{b}(h)$ is determined starting from the ETSs sequence. Specifically, starting from
316 a given storm sequence, the related ETSs sequence is determined by calculating for each
317 event the intensity and duration parameters a and b of the ETS. Then two different



318 assumptions can be made. The simplest is to consider an average value of b , in other words to
 319 assume a constant base-height regression. The other is to calculate a linear or exponential
 320 regression function. In general, the function $\bar{b}(h)$ presents a decaying pattern, because of
 321 which, an exponential function is preferable in order to guarantee positive values of the base
 322 b for any storm threshold. To calculate the regression, initially the data have to be divided in
 323 classes of triangle height and then for each class the average values of a and b have to be
 324 calculated. Then the regression may be easily determined representing data in a Cartesian plot
 325 with parameters b in y axis and parameter a in x axis respectively. By fitting the data by
 326 means of an exponential law as per the relationship given below:

$$327 \quad \bar{b}(a) = k_1 \exp(k_2 a) \quad (15)$$

328 where k_1 (hours) and k_2 (m^{-1}) are parameters depending on the storms characteristics at the
 329 considered site.

330 The determination of the base-height regression function despite very simple from a
 331 computational and mathematical point of view, requires careful attention because of its
 332 sensibility to the time interval between the data of H_s used in the analysis. In this regard, it is
 333 worth noting that ETS duration parameter b , is strongly dependent on the actual storm
 334 structure close to the storm peak. Specifically it tends to increase as the storm structure
 335 became flat and it is quite small for steep storms. When data sampling interval is more than
 336 one to three hours, one may have very flat storms. This involves that the calculation may lead
 337 to big values of duration b . This aspect causes that return values of H_s may be underestimated
 338 (Arena et al., 2013). This aspect strongly affect predictions when wave model data are
 339 processed (3 to 6 hours between two successive data of H_s). To overcome this problem, a
 340 good practice is to do the analysis in conjunction with buoy data close to the location under
 341 study. In these cases, the base height regression function calculated from buoys is utilized for
 342 correcting the base height regression function obtained from model data.

343 Concerning the distribution of the significant wave height $P(H_s > h)$, three-parameters
 344 Weibull distribution is considered.

$$345 \quad P(H_s > h) = \exp \left[- \left(\frac{h - h_l}{w} \right)^u \right] \quad (16)$$



346 where u , h_l and w are the characteristic parameters at the considered location. In particular u
347 and h_l are the shape parameters and w is the scale parameter of the distribution.

348 **4. Results**

349 In this study, hindcast results for ERA-interim data are compared with buoy measurements
350 for different estimation models. Further study of the various uncertainties due to the
351 parameter estimation method, the sample size, sample interval and location conditions
352 involved in this analysis are also examined.

353 **4.1 GEV analysis**

354 In the application of generalised extreme value distribution to the sampled annual maxima
355 data, the scale, shape and location parameters can be used to make statements about the
356 probability of the annual maximum exceeding a particular level. A change in either parameter
357 can affect the long-period return levels.

358

359 The parameter estimation is done by maximum likelihood estimate method (MLE) and
360 probability weighted moments (PWM) method (Hosking et al., 1985) and resulted parameters
361 are shown in Table 2. It has been observed that the shape parameter is positive for ERA-
362 interim data indicating that this data would follow Frechét distribution and the tail of the
363 cumulative distribution function decreases more slowly.

364 The influence of estimated parameters in fitting the data to the GEV model is presented in
365 Fig. 3a. It shows the level of fitting of the empirical CDF with the GEV PWM and GEV
366 MLE models. The difference in the normal coordinates in their fitting with empirical CDF is
367 insignificant. Figure 3b shows the variation in tail estimates of the PWM and MLE parameter
368 estimation methods in logarithmic scale. The results show for both buoy and ERA-interim
369 data sets, the PWM method of parameter estimation yields better estimates compared to the
370 MLE method.

371 The statistical parameter, root mean square error was estimated in order to check the level of
372 fitting of sampled data to the GEV distribution model. The root mean square error is a
373 residual between the empirical cumulative distribution obtained from the actual observed data
374 and the theoretical GEV model cumulative distribution. Lower the value of RMSE i.e., near
375 to zero indicates a better fit of sampled data to the GEV distribution model. The fitting of
376 GEV to buoy and ERA-interim data is found to be good for both PWM and MLE methods.



377 The variation RMSE value of the MLE estimates is usually smaller than those of the PWM
378 estimates for both buoy and ERA-interim data.

379 **4.2 GPD analysis**

380 In POT method, the selection of a suitable threshold value is the key in achieving a robust
381 sample data set. The mean residual plot, between the mean excess GPD and threshold helps
382 in determining a proper range of threshold to be selected (Coles, 2001). Such plots with 95%
383 confidence for the data ERA IN-1, (Fig. 4) appear to have two slopes with major transition at
384 the threshold range of 1.5 to 2.5 indicates the range of threshold could possibly be selected.
385 However, attention should be made as too high threshold can results in less sampled data set
386 which results in a higher variance of the GPD model.

387 The sample used in the peaks over threshold method has to be extracted in such a way that
388 the data can be modelled as independent observations. A process of de-clustering helps
389 collecting only the peaks within the clusters of successive exceedances of a specified
390 threshold and are retained in such a way that they are sufficiently apart (so that they belong to
391 'independent storms'). Specifically, in the present applications we have treated cluster
392 maxima at a distance of less than 48 hours apart as belonging to the same cluster (Caires,
393 2011). Table 3 provides the selected threshold and the number of exceedances of that
394 specified threshold with 48h interval. It is seen that the threshold values are observed to be
395 dependent on the length, location and interval of the datasets. The major factor has to be the
396 location, since the higher latitude locations are exposed to more severe wave and wind
397 conditions than those at the lower latitudes.

398 For parameter estimation, the PWM and MLE methods are used. The MLE has a
399 considerable statistical motivation but can turn out to be poor estimators, especially in the
400 case where the number of estimated parameters is large. So the approach chosen here was to
401 utilize a variety of techniques like PWM and MLE for exploratory fitting for the probability
402 model and chose the best possible parameters.

403 To verify the estimated parameters for the GPD model, quantile-quantile (QQ) plots were
404 used. In Fig. 5a, the QQ plots for the dataset NOAA44005 is shown, comparing the estimated
405 GPD with the sample data for PWM parameter estimation method. In order to check the
406 influence of parameters resulting from PWM and MLE parameter estimation models, the
407 Root mean square error was estimated for GPD model also and presented in Table 3.



408

409 Comparing the estimates and the fits, one can conclude that the MLE fits seem less adequate
410 and that the shape parameter estimates are lower than those of the PWM fits. These results
411 support the recommendations of Hosking et al., 1985 to preferably use the PWM method for
412 GPD or GEV estimation from relatively short duration of data with limited heavy-tailed
413 cumulative distributions. Figure 5b shows the return value GPD plot of PWM fit to the
414 dataset NOAA44005.

415

416 **4.3 Polynomial approximation method analysis**

417 Polynomial approximation (P-approximation) method has a distinct advantage of selecting
418 the optimum choice of the parameters N_S , N_T , and n . The detailed analysis demonstrates that
419 all approximation parameters (n , N_T , and N_S) are equally important. Figure 6 shows the
420 application of P-approximation method for both buoy and ERA-interim data at Alghero buoy
421 station. In the above mentioned figure, the bottom level ($\ln(1-F) = -12.6$) indicates probability
422 of occurrence once for 100 years and can be deduced by Eq. 12 with discrete of data
423 observations of 3hr interval. For 1hr and 6hr interval of data observations, the probability of
424 occurrence once in 100 years can be obtained as -13.7 and -11.9 respectively.

425 One can see the adaptation of P-approximation to the real behavior of the tails for provision
426 functions. For the Alghero location buoy data, the optimized parameters obtained are $N_S=0$,
427 $N_T=8$ (points used for approximation), $n=2$ (degree of approximation function) to arrive at the
428 optimum return value as shown in the Fig. 6.

429 The optimum choice of parameters will also depend on standard deviation δ (Eq. 13) which
430 resembles the residual between the actual tail of the provision function and the Polynomial
431 approximation tail fitted to it. Lower the value of δ i.e., near to zero indicates a better fit
432 between actual tail of the provision function and the Polynomial approximation tail fitted.
433 The parameters N_S , N_T , and n for all the datasets including the resulted standard error δ are
434 provided in Table 4.

435 **4.4 Analysis of ETS Model**

436 The calculation of the 100 yrs return values via ETS model is done by means of Eq. (13),
437 known the base-height regression function Eq. (14) and the probability distribution Eq. (15)
438 of H_s at the examined location. The base height regression function is determined starting
439 from the storm sequence at the considered site, while the probability distribution is achieved



440 processing the whole data set of H_s . An important aspect to be taken into account in
441 estimating the parameters of both Eq. (14) and Eq. (15) is the time interval between two
442 successive data of H_s . A value of 3-6 hours should be appropriate for estimating the
443 parameters of the probability distribution, in order to guarantee the stochastic independence
444 between successive events, but could be too high for determining the parameters of the base-
445 height regression function.

446 In fact, Arena et Al., 2013 has shown that as the time interval between two successive H_s ,
447 increases, the peak of the storm may not be well identified, involving flat storm history that
448 led to an increase of the duration b of ETSs respect to the case with lower time interval
449 between H_s data. Such situation are those of wave model data. In this paper both wave model
450 and buoy data are considered.

451 To determine the base-height regression function parameters, the actual storm sequence is
452 identified starting from H_s time series, and for each actual storm the parameters a and b of
453 ETS are calculated (Boccotti, 2000). Then the ETS are divided into classes of H_s of 1m width
454 and the average value a_m and b_m of a and b for each class is considered. The sequence a_m, b_m
455 is plotted in a Cartesian diagram and fitted by an exponential law as the Eq. (14). For the case
456 of wave model data a further step is required. Specifically, considering an increase of b due to
457 high time interval between H_s data, the regression should be corrected considering a reducing
458 factor r , defined as the ratio between the average values of the base calculated starting from
459 buoy data moored close to the considered site and the average value calculated by means of
460 wave model data. The regression parameters k_1 and k_2 at each considered site are summarized
461 in Table 5 in conjunction with the parameters u, w and h_l of the probability distribution Eq.
462 (15).

463 5. Discussions

464 From the results it is observed that the estimates from buoy observations are higher compared
465 to the estimates for ERA-interim datasets. This trend is being observed from all the
466 estimation models. Shanas and kumar, 2014 have found that at certain location in Arabian sea
467 the maximum H_s based on ERA dataset in deep water is about 15% less than that of buoy
468 measured data. Herein, also a similar phenomenon of variation of 20-30% while comparing
469 maximum observed H_s of Buoy data and ERA-interim at NOAA440050, NOAA46050 and
470 Alghero buoy locations is observed. This in turn will result in under estimation of return
471 value of ERA interim data.



472

473 The under prediction of ERA interim data suggests, that high wave events mainly due to the
474 cyclone events are difficult to capture by ECMWF numerical model. It is a familiar
475 phenomenon and challenge that the smoothing effect implanted in numerical model will lead
476 to the flattened variability at relatively high frequencies, resulting in the missing peaks. An
477 additional potential explanation for the under prediction is that the simulated ERA-Interim
478 data contains 6- hourly intervals of H_s data. It is possible because of the lower sampling rate,
479 the maximum wave heights in a storm occurs between observations will not be recorded. To
480 overcome this, it is obvious that ECMWF numerical modeling system need further
481 improvement in correction or calibration of the ERA-interim data especially when this
482 hindcast is used for the extreme wave analysis.

483

484 Final results on the 30,100 year extreme wave estimates, obtained by the GEV, GPD, ETS
485 and Polynomial approximation methods described above are presented in Table 6 and 7. The
486 variation of these estimates from the measured maximum wave heights will give a statistical
487 validation of the performance of the estimation models. The percentage of variation of 30-yr
488 and 100-yr return value estimates from measured 36 year maximum wave height are
489 calculated for this analysis. Here one can observe the following principal peculiarities from
490 the results of above mentioned statistical validation methodology.

491

492 The GEV and GPD methods, shows the 30 year return values smaller than the measured
493 maximum H_s for all the locations mostly by an extent of 10-25%. In the cases of simulated
494 data these models exhibit high deviations from measured maximum H_s . This peculiarity is
495 because of the reason of neglecting the behavior of the tails for provision functions, accepted
496 in GEV and GPD methods. As a result, this leads to underestimating the return values. This is
497 a reasonable shortage of these methods, as far as one cannot forecast extreme smaller return
498 values than ones observed already.

499

500 The GEV model with annual maxima sample resulted in over estimation of return values
501 compared to the GPD model with peaks over threshold approach. As the GEV estimation
502 model considers only the highest H_s in the year, which might lead to the overestimation of
503 Annual maxima based approach in comparison with the other method. For most of the
504 locations, there is not much variation in the results of the PWM, MLE parameter estimated
505 GEV and GPD models. But Hosking et al., 1985 recommended to always applying the PWM



506 parameter estimation method for GPD and GEV distribution models from relative short
507 datasets with not too heavy-tailed distributions. Furthermore, PWM works for a wider range
508 of parameter values than MLE method.

509

510 The results from the P-method are remarkably closer to the measured maximum values than
511 those obtained by the GEV, GPD and ETS method, which variation is as high as 5% to as
512 less as -7%. The Polynomial approximation method shows consistency in 100-yr estimated
513 return values for both simulated and buoy wave height datasets, as these varies consistently
514 between 7-13% from the measured maximum values. GEV, GPD and ETS methods fails in
515 the above mentioned criterion as variation is as high as 56% to as low as -19% which are not
516 possible in nature.

517

518 This consistency of polynomial approximation method estimates is due the dependence of
519 return values on the actual kind of the tail for provision function, which could vary and is
520 dependent on the sample of the series. The only disadvantage of P-app method ($F_{ap}(H_s, n)$) is
521 the necessity to control reliability of its extrapolation, as far as the extrapolation of
522 polynomial with the order $n > 1$ may have twists and extremes. This well-known fact could
523 be provided by a considerable variability of the "tail" for $F(W)$. Such an extrapolation is
524 implausible, of course. Therefore, it is necessary to vary the parameters N_S , N_T , and the order
525 of polynomial n in such a manner, the twists of extrapolation could be avoided.

526 **6. Conclusions**

527 In this study we chose the simulated ERA-Interim wave data, for the two following reasons.
528 First, they have more regular coverage for the whole World ocean, and the Indian coast, in
529 particular. Second, numerical simulated datasets have long and regular continuous series,
530 what is very important for the extreme value statistical aims.

531 This study focused on the estimation of the extreme significant wave heights only. The
532 analyses carried out and results produced will aid in the preparation of a 100 year extreme
533 wave map for the Indian water domain which may serve as a quick guide to identify regions
534 where extremes lie within the design criteria of the coastal and offshore structures to be
535 constructed.

536 We have considered four different approaches to the return values estimating: the GEV
537 distribution model based on annual maxima sample, the GPD distribution model based on



538 peaks over threshold sample, ETS model based on storms and the polynomial approximation
539 method for the tail of provision function. All of them have their own advantages and
540 shortages.

541 The main shortage of the GEV and GPD methods are the high variation in underestimating or
542 overestimating return values with respect to ones presenting in the time-series. The shortage
543 of the P-app method is related to the ambiguity of the return values estimations, obtained
544 from different parts of the full time-series. It is also found that the values estimated based on
545 GEV model were slightly larger than those from the GPD. But GPD method with peaks over
546 threshold sample is preferable in the locations of multiple storm events in a single year. In
547 turn, the estimates through the Polynomial approximation method, depend on the actual kind
548 of the tail for provision function, which could vary and is dependent on the sample of the
549 series resulted in showing the consistency in 100-yr estimated return values for both
550 simulated and buoy wave height datasets, as these varies consistently between 7-13% from
551 the measured maximum values.

552 It is observed that the return value estimates from buoy observations are higher when
553 compared to the estimates for ERA-interim datasets. The under prediction of ERA interim
554 data suggests, that high wave events mainly due to the cyclone events are difficult to capture
555 by ECMWF numerical model. To overcome this, it is obvious that ECMWF numerical
556 modeling system need further improvement in correction or calibration of the ERA-interim
557 data especially when this hindcast is used for the extreme wave analysis.

558 **Acknowledgments**

559 This paper has been developed during the Marie Curie IRSES project “Large Multi- Purpose
560 Platforms for Exploiting Renewable Energy in Open Seas (PLENOSE)” funded by European
561 Union (Grant Agreement Number: PIRSES-GA-2013-612581).

562 This work was partially supported by the joint Russian-Indian (RFBR-DST) grant, # 14-05-
563 92692-Ind-a.

564 **References**

565 Anderson, C. W., D. J. T. Carter, and P. D. Cotton, 2001: Wave climate variability and
566 impact on offshore design extremes. Shell International and the Organization of Oil and Gas
567 Producers Rep., 99 p.



- 568 Arena, F. & Pavone, D. (2006) The return period of non-linear high wave crests, *Journal of*
569 *Geophysical Research*, Vol. 111, No. C8, paper C08004, doi: 10.1029/2005JC003407
- 570 Arena, F. & Pavone, D. (2009) A generalized approach for the long-term modelling of
571 extreme sea waves, *Ocean Modelling*, Vol. 26, Issue 4, pp. 217-225.
572 doi:10.1016/j.ocemod.2008.10.003
- 573 Arena, F., Laface, V., Barbaro, G., Romolo, A., 2013. Effects of sampling between data of
574 significant wave height for intensity and duration of severe sea storms, *International Journal*
575 *of Geosciences*, Vol. 4, Issue 1A, pp. 240-248 doi:10.4236/ijg.2013.41A021.
- 576 Arena F., Laface V., Malara G., Romolo A., Viviano A., Fiamma V., Sannino G., Carillo A.,
577 2015. Wave climate analysis for the design of wave energy harvesters in the Mediterranean
578 Sea, *Renewable energy*, volume 77, pp. 125-141, ISSN: 0960-1481.
- 579 Berrisford, P., Dee, K., Fielding, M., Fuentes, P., Kalberg, S., Kobayashi, and S. Uppala, The
580 ERA-Interim Archive. ERA report series, 2009(1): p. 1-16.
- 581 Boccotti, P., 1986. On coastal and offshore risk analysis. Excerpta of the Italian Contribution
582 to the Field of Hydraulic Eng., 19–36.
- 583 Boccotti, P., 2000. *Wave mechanics for ocean engineering*. Elsevier, Amsterdam, The
584 Netherlands, 496 pp.
- 585 Castillo, E., 1988: *Extreme value theory in Engineering*. Academic Press, 389 pp.
- 586 Coles, S., 2001: *An Introduction to Statistical Modeling of Extreme Values*. Springer-Verlag,
587 208 pp.
- 588 Davidson & Smith (1990), *Models for Exceedances over high Thresholds*, *Journal of the*
589 *Royal Statistical Society B*, 52, pp. 393-442. Grimshaw, S. D. (1993)
- 590 Dee, D. and S. Uppala, Variational bias correction in ERA-Interim2008: ECMWF.
- 591 Fedele, F., and Arena, F., 2010. The equivalent power storm model for long-term predictions
592 of extreme wave events. *J. Phys. Oceanogr.* 40, 1106–1117.
- 593 Ferreira, J.A., and C. Guedes Soares, 1998: An application of the peaks over threshold
594 method to predict extremes of significant wave height. *J. Offshore Mech. Arct. Eng.*, 120,
595 165–176.



- 596 Ferreira, J. A., and C. Guedes Soares, 2000: Modelling distributions of significant wave
597 height. *Coast. Eng.*, 40, 361–374.
- 598 Goda Y. Statistical analysis of extreme waves (Chapter 11). In: *Random seas and design of*
599 *maritime structures*, 15th volume of advanced series on ocean engineering, World Scientific
600 Publishing Co., 2000; 377- 425.
- 601 Hosking, J.R.M, Wallis, J.R. and Wood E.F. (1985), Estimation of the generalized extreme-
602 value distribution by the method of probability-weighted moments *Technometrics* (27), pp.
603 251-261
- 604 Jiangxia Li, Yongping Chen, Shunqi Pan, Yi Pan, Jiayu Fang, Derrick M.A. Sowa,
605 Estimation of mean and extreme waves in the East China Seas, *Applied Ocean Research*
606 56(2016) 35-47.
- 607 Laface, V. and Arena, F., (2016), A new equivalent exponential storm model for long-term
608 statistics of ocean waves, *Coastal Engineering*, Volume 116, Pages 133-151.
- 609 Liberti, L., Carillo, A., Sannino, G., (2013), Wave energy resource assessment in the
610 Mediterranean, the Italian perspective. *Renewable Energy*; 50: 938-49.
- 611 Lionello, P., H. Gunther, and P. A. E. M. Janssen. 1992. Assimilation of altimeter data in a
612 global third-generation wave model. *J. Geophys. Res.* 97(C9):14453–14474.
- 613 Massel RS (1978) Needs for Oceanographic Data to Determine Loads on Coastal and
614 Offshore Structures. *IEEE Journal of Oceanic Engineering* vol oe-3 no. 4.
- 615 Neelamani, S., (2009), Influence Of threshold value on Peak Over Threshold Method on the
616 predicted extreme significant wave heights in Kuwaiti territorial waters. *J. Coast. Res.*,
617 Special Issue 56 564-568.
- 618 P.R.Shanas and V. Sanilkumar, Comparison of ERA-Interim waves with buoy data in eastern
619 Arabian sea during high waves, *Indian journal of Marine sciences* vol.43(7), July 2014,pp.
- 620 Sofia Caires (2011),Extreme value analysis: wave data, *JCOMM Technical Report No. 57*
- 621 N.V. Teena, V. Sanil Kumar, K. Sudheesh, R. Sajeev, Statistical analysis on Extreme wave
622 Height, *Natural Hazards*, vol.64; 2012; 223-236.



- 623 V.G. Polnikov and I.A. Gomorev, On Estimating the return values for time series of wind
624 speed and wind wave height, ISSN 1068-3739, Russian Meteorology and Hydrology, 2015,
625 Vol. 40, No. 12, pp. 820–827. Ó Allerton Press, Inc., 2015.
- 626 Vicinanza, D., Contestabile, P. & Ferrante, V., (2013), Wave energy potential in the north-
627 west of Sardinia (Italy). Renewable Energy 50: 506-521.



628

Table 1: ERA-Interim data locations and Buoy stations

| Data Point | Coordinates | Availability | Interval (Hr) | No. of data points |
|--------------------|--------------------------|---------------------|----------------------|---------------------------|
| <i>ERA IN-1</i> | <i>19.50N, 85.75E</i> | 1979-2014 | 6 | 52596 |
| <i>ERA IN-2</i> | <i>15.50N, 81.00E</i> | 1979-2014 | 6 | 52596 |
| <i>ERA IN-3</i> | <i>10.25N, 75.75E</i> | 1979-2014 | 6 | 52596 |
| <i>ERA IN-4</i> | <i>14.50N, 73.50E</i> | 1979-2014 | 6 | 52596 |
| <i>NDBC 44005</i> | <i>43.204N, 69.128W</i> | 1978-2014 | 1 | 254221 |
| <i>ERA 44005</i> | <i>43.25N, 69.125W</i> | 1979-2014 | 6 | 52596 |
| <i>NDBC 46050</i> | <i>44.656N, 124.526W</i> | 1991-2014 | 1 | 180231 |
| <i>ERA 46050</i> | <i>44.625N, 124.50W</i> | 1991-2014 | 6 | 35064 |
| <i>RON Alghero</i> | <i>40.548N, 8.107E</i> | 1989-2008 | 3 | 125443 |
| <i>ERA Alghero</i> | <i>40.5N, 8.125E</i> | 1989-2008 | 6 | 29220 |

629



630

Table 2: PWM and MLE parameter estimators fitting GEV

| Data | PWM method | | | | MLE method | | | |
|--------------------|------------|--------|----------|-------|------------|--------|----------|-------|
| | ξ | μ | σ | RMSE | ξ | μ | σ | RMSE |
| <i>ERA IN-1</i> | 0.1125 | 3.1523 | 0.3849 | 0.053 | 0.1157 | 3.1572 | 0.3779 | 0.045 |
| <i>ERA IN-2</i> | 0.2085 | 1.9181 | 0.3108 | 0.081 | 0.4971 | 1.8838 | 0.2499 | 0.039 |
| <i>ERA IN-3</i> | 0.0311 | 2.8386 | 0.3279 | 0.032 | 0.0296 | 2.8413 | 0.3270 | 0.035 |
| <i>ERA IN-4</i> | 0.1169 | 3.6889 | 0.4553 | 0.033 | 0.1118 | 3.6975 | 0.4485 | 0.029 |
| <i>NOAA 44005</i> | -0.1642 | 6.7735 | 1.0880 | 0.052 | -0.1811 | 6.7958 | 1.0571 | 0.023 |
| <i>ERA 44005</i> | -0.0866 | 5.0506 | 0.5649 | 0.031 | 0.0457 | 5.0706 | 0.5741 | 0.030 |
| <i>NOAA 46050</i> | -0.1190 | 8.9863 | 1.5655 | 0.052 | -0.1038 | 8.9429 | 1.6407 | 0.039 |
| <i>ERA 46050</i> | -0.0251 | 7.1700 | 0.7646 | 0.047 | 0.0554 | 7.1705 | 0.7268 | 0.051 |
| <i>RON Alghero</i> | -0.5089 | 7.4373 | 1.4405 | 0.112 | -0.4992 | 7.4498 | 1.3588 | 0.043 |
| <i>ERA Alghero</i> | 0.0746 | 5.555 | 0.6298 | 0.069 | -0.0874 | 5.5719 | 0.6003 | 0.061 |

631



632

Table 3: PWM and ML parameter estimators fitting GPD

| Data | Threshold μ | No. of exceedence | PWM method | | | MLE method | | |
|--------------------|--------------------|----------------------|------------|---------|-------|------------|---------|-------|
| | | | σ | ξ | RMSE | σ | ξ | RMSE |
| <i>ERA IN-1</i> | 2.5 | 153 | 0.4429 | 0.0415 | 0.028 | 0.4489 | 0.0286 | 0.026 |
| <i>ERA IN-2</i> | 1.5 | 160 | 0.2515 | 0.1438 | 0.045 | 0.2471 | 0.1588 | 0.052 |
| <i>ERA IN-3</i> | 2.5 | 107 | 0.3350 | -0.0485 | 0.036 | 0.3149 | 0.0143 | 0.025 |
| <i>ERA IN-4</i> | 3.0 | 154 | 0.5428 | -0.0651 | 0.035 | 0.5200 | -0.0206 | 0.025 |
| <i>NOAA 44005</i> | 5.0 | 227 | 1.3147 | -0.1677 | 0.055 | 1.3396 | -0.1892 | 0.063 |
| <i>ERA 44005</i> | 4.0 | 190 | 0.7335 | -0.1159 | 0.201 | 0.6938 | -0.0560 | 0.025 |
| <i>NOAA 46050</i> | 6.0 | 232 | 1.4608 | -0.0200 | 0.019 | 1.5058 | -0.0514 | 0.031 |
| <i>ERA 46050</i> | 5.0 | 203 | 1.5480 | -0.3879 | 0.126 | 1.2886 | -0.1654 | 0.066 |
| <i>RON Alghero</i> | 5.0 | 153 | 1.6541 | -0.2957 | 0.100 | 1.6110 | -0.2614 | 0.089 |
| <i>ERA Alghero</i> | 4.0 | 128 | 0.9342 | -0.1474 | 0.053 | 0.9642 | -0.1835 | 0.066 |

633



634

Table 4: Selection of optimum values of approximation parameters

| Data | No. of points used for approximation N_T | n | δ |
|--------------------|--|----------|----------------------------|
| <i>ERA IN-1</i> | 6 | 2 | 0.176 |
| <i>ERA IN-2</i> | 6 | 3 | 0.044 |
| <i>ERA IN-3</i> | 5 | 3 | 0.032 |
| <i>ERA IN-4</i> | 7 | 3 | 0.063 |
| <i>NOAA 44005</i> | 8 | 2 | 0.118 |
| <i>ERA 44005</i> | 7 | 1 | 0.197 |
| <i>NOAA 46050</i> | 5 | 2 | 0.026 |
| <i>ERA 46050</i> | 6 | 1 | 0.200 |
| <i>RON Alghero</i> | 8 | 2 | 0.100 |
| <i>ERA Alghero</i> | 7 | 2 | 0.105 |

635



636 **Table 5:** Base-height regression parameters k_1 , k_2 calculated considering a storm sample with
 637 actual durations greater or equal to 18 hours, probability distribution parameters u , w and h_l .

| Data | u | w [m] | h_l [m] | k_1 [h] | k_2 [m ⁻¹] |
|--------------------|-------|---------|-----------|-----------|--------------------------|
| <i>ERA IN-1</i> | 1.320 | 0.714 | 0.459 | 397.61 | -0.251 |
| <i>ERA IN-2</i> | 0.773 | 0.142 | 0.481 | 255.73 | -0.097 |
| <i>ERA IN-3</i> | 1.600 | 0.851 | 0.488 | 348.02 | -0.086 |
| <i>ERA IN-4</i> | 1.504 | 1.099 | 0.498 | 397.6 | -0.159 |
| <i>NDBC 44005</i> | 1.121 | 1.150 | 0.409 | 76.125 | 0.0308 |
| <i>ERA 44005</i> | 1.141 | 0.884 | 0.461 | 114.05 | -0.071 |
| <i>NDBC 46050</i> | 1.333 | 1.945 | 0.480 | 154.9 | -0.101 |
| <i>ERA 46050</i> | 1.625 | 2.321 | 0.000 | 106.94 | -0.055 |
| <i>RON Alghero</i> | 1.155 | 1.299 | 0.000 | 318.37 | -0.235 |
| <i>ERA Alghero</i> | 1.227 | 1.157 | 0.000 | 135.53 | -0.035 |

638



639

Table 6: 30 year return value estimates (m)

| Data | Measured maximum | GEV | | GPD | | P-App | ETS |
|--------------------|------------------|------|------|------|------|-------|------|
| | | PWM | MLE | PWM | MLE | | |
| <i>ERA IN-1</i> | 4.91 | 4.8 | 4.8 | 4.9 | 4.8 | 4.6 | 4.7 |
| <i>ERA IN-2</i> | 3.59 | 3.5 | 4.1 | 3.3 | 3.4 | 3.6 | 3.3 |
| <i>ERA IN-3</i> | 4.83 | 4.0 | 4.0 | 3.9 | 4.1 | 4.6 | 4.3 |
| <i>ERA IN-4</i> | 6.17 | 5.6 | 5.5 | 5.1 | 5.5 | 5.9 | 5.9 |
| <i>NOAA 44005</i> | 10.10 | 9.6 | 9.5 | 9.5 | 9.4 | 10.6 | 9.9 |
| <i>ERA 44005</i> | 8.27 | 7.3 | 7.2 | 6.5 | 7.0 | 7.9 | 8.0 |
| <i>NOAA 46050</i> | 14.05 | 13.7 | 13.4 | 12.4 | 12.3 | 14.1 | 12.8 |
| <i>ERA 46050</i> | 10.93 | 9.9 | 9.9 | 8.0 | 9.0 | 10.2 | 9.5 |
| <i>RON Alghero</i> | 9.88 | 9.8 | 9.7 | 9.4 | 9.5 | 9.2 | 10.3 |
| <i>ERA Alghero</i> | 7.51 | 7.5 | 7.4 | 6.6 | 6.9 | 7.6 | 7.4 |

640



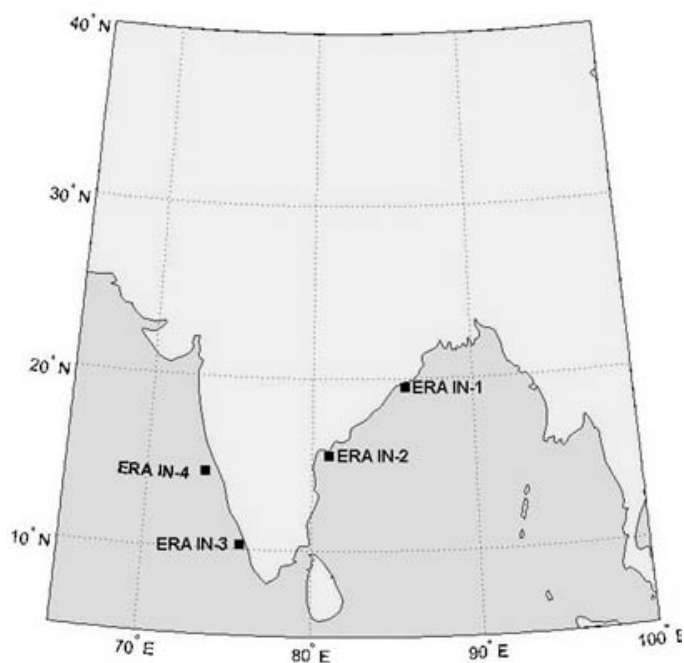
641

Table 7: 100 year return value estimates (m)

| Data | Measured maximum | GEV | | GPD | | P-App | ETS |
|--------------------|------------------|------|------|------|------|-------|------|
| | | PWM | MLE | PWM | MLE | | |
| <i>ERA IN-1</i> | 4.91 | 5.5 | 5.5 | 5.65 | 5.5 | 4.8 | 5.1 |
| <i>ERA IN-2</i> | 3.59 | 4.3 | 5.6 | 4.0 | 4.1 | 4.0 | 3.6 |
| <i>ERA IN-3</i> | 4.83 | 4.5 | 4.5 | 4.2 | 4.4 | 4.7 | 4.4 |
| <i>ERA IN-4</i> | 6.17 | 6.5 | 6.6 | 5.6 | 6.0 | 6.4 | 6.1 |
| <i>NOAA 44005</i> | 10.10 | 10.3 | 10.1 | 10.1 | 10.0 | 11.4 | 10.7 |
| <i>ERA 44005</i> | 8.27 | 8.3 | 8.0 | 7.2 | 7.9 | 9.0 | 8.4 |
| <i>NOAA 46050</i> | 14.05 | 15.1 | 14.6 | 14.2 | 14.1 | 15.2 | 13.8 |
| <i>ERA 46050</i> | 10.93 | 10.9 | 11.0 | 8.9 | 9.8 | 11.3 | 11.1 |
| <i>RON Alghero</i> | 9.88 | 10.1 | 10.0 | 9.9 | 10 | 9.7 | 12.5 |
| <i>ERA Alghero</i> | 7.51 | 8.5 | 8.0 | 7.7 | 8.0 | 8.2 | 8.7 |

642

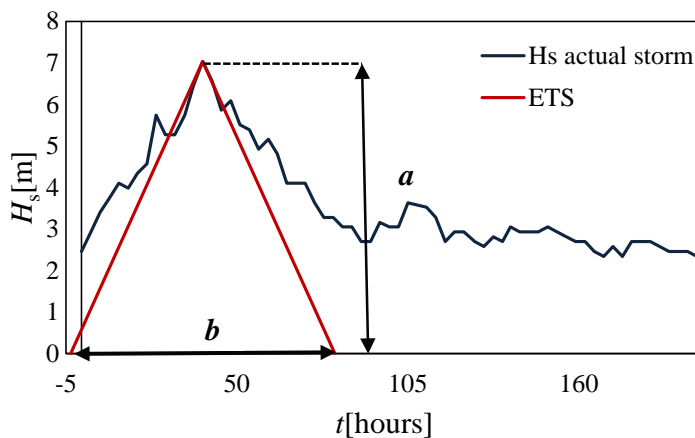
643



644

645

Figure 1: Locations along the Indian coast



646

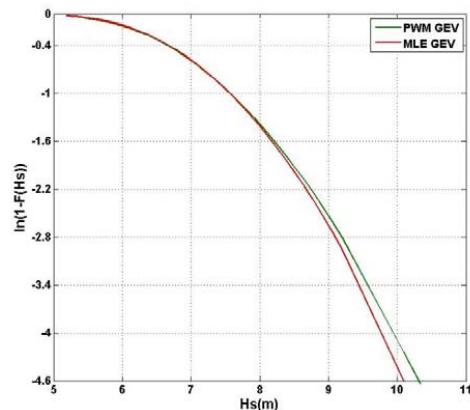
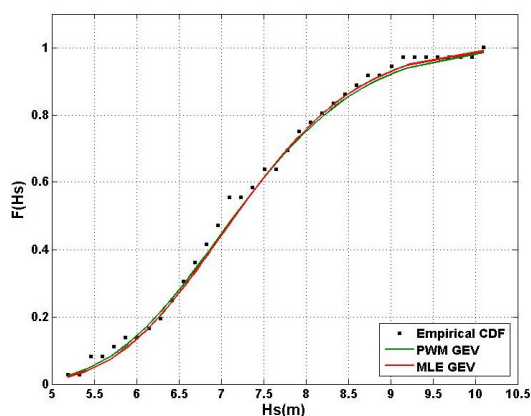
647

648

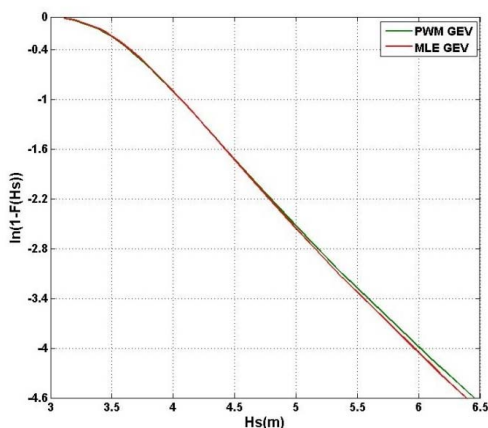
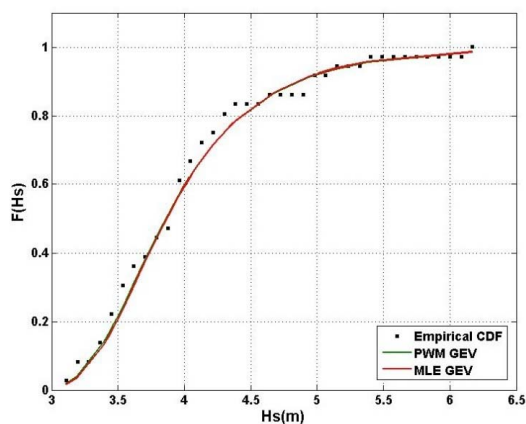
Figure 2: Typical representation of actual storm and associated ETS.



649



650



651

(a)

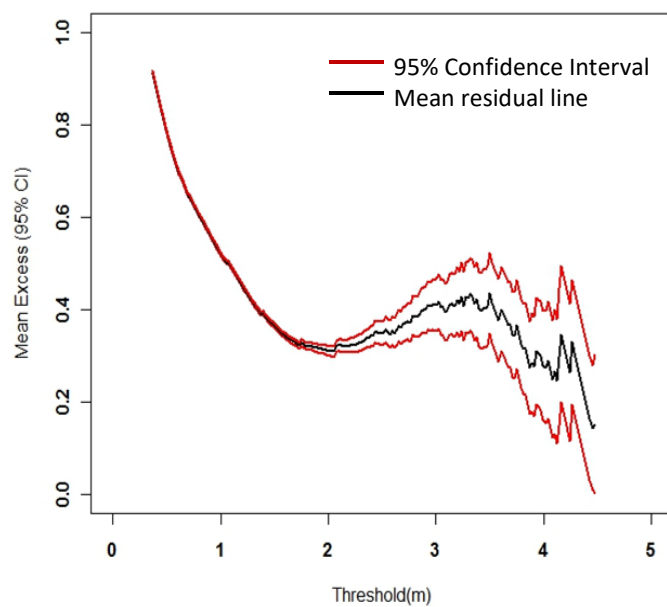
(b)

652

653

654

Figure 3:(a) Comparison of GEV model CDF to the empirical CDF for NOAA44005 and ERA IN-4 (b) Variation of tail GEV model CDF in logarithmic coordinates for NOAA44005 and ERA IN-4

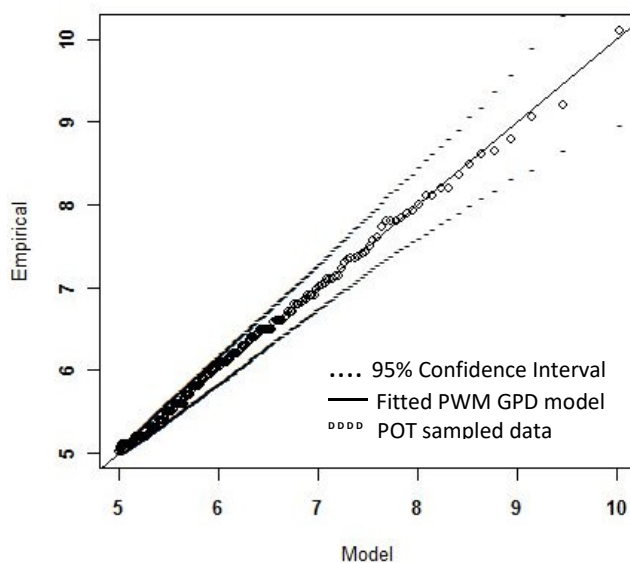


655

656

Figure 4: Mean Residual plot of ERA IN-1 with 95% confidence limits

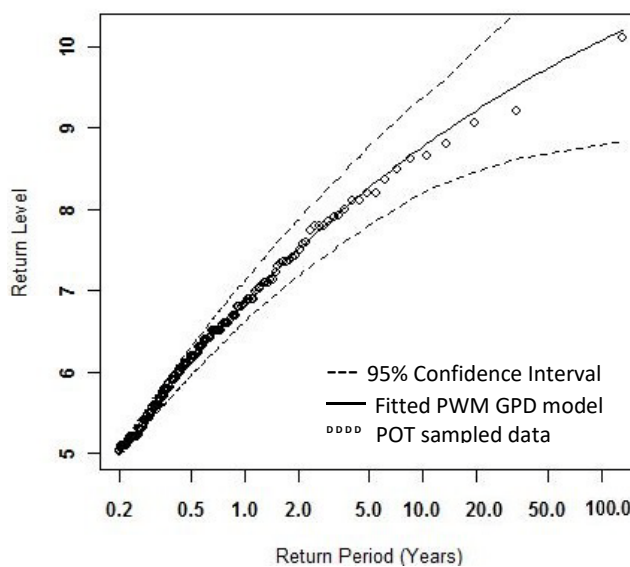
657



658

659

(a)

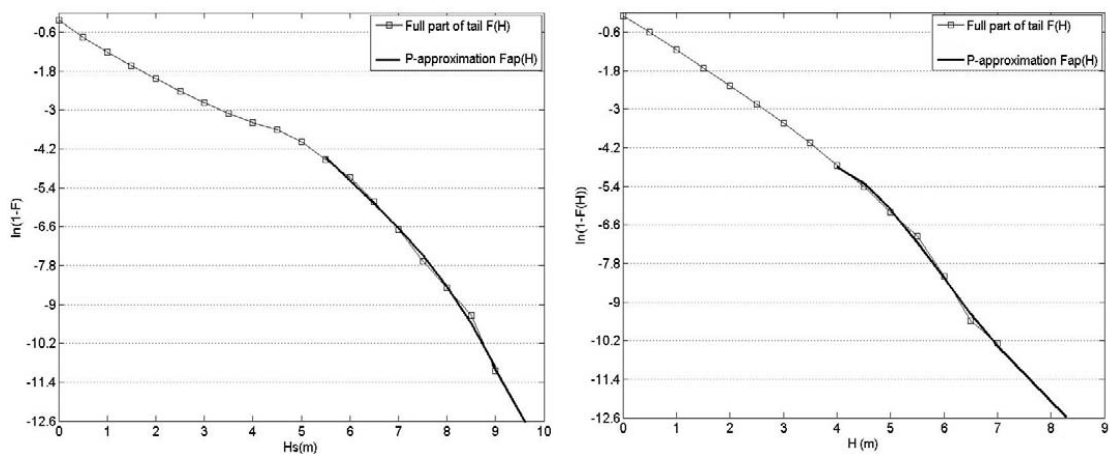


660

661

(b)

662 **Figure 5 :**(a) Quantile-Quantile plots of GPD model for NOAA44005 data (b) Return level
663 plots of GPD model for NOAA44005 data.



664

665 **Figure 6:** P-approximation for series of wave heights H_s at Alghero buoy station for Buoy
666 and ERA-interim datasets